Mapping the ECG in the live rabbit heart using Ultrasound Current Source Density Imaging with coded excitation

Yexian Qin[1], Qian Li[1], Pier Ingram[1], and Russell S. Witte[1]

[1]Department of Medical Imaging, University of Arizona, Tucson, AZ USA 85724
rwitte@email.arizona.edu

Abstract: **Ultrasound current source density imaging (UCSDI) is a noninvasive technique for mapping electric current fields in 4D (space + time) with the resolution of ultrasound imaging. This approach can potentially overcome limitations of conventional electrical mapping procedures often used during treatment of cardiac arrhythmia or epilepsy. However, at physiologic currents, the detected acoustoelectric (AE) interaction signal in tissue is very weak. In this work, we evaluated coded ultrasound excitation (chirps) for improving the sensitivity of UCSDI for mapping the electrocardiogram (ECG) in a live rabbit heart preparation. Results confirmed that chirps improved detection of the AE signal by as much as 6.1 dB compared to a square pulse. We further demonstrated mapping the ECG using a clinical intracardiac catheter, 1 MHz ultrasound transducer and coded excitation. B-mode pulse echo and UCSDI revealed regions of high current flow in the heart wall during the peak of the ECG. These improvements to UCSDI are important steps towards translation of this new technology to the clinic for rapidly mapping the cardiac activation wave.**

Index Term: **acoustoelectric, cardiac arrhythmia mapping, ECG, coded excitation chirps**

I. INTRODUCTION

Epilepsy and cardiac arrhythmia are serious health problems affecting millions of patients around the world. Resynchronization and ablation therapy are common treatments for cardiac arrhythmias and neurological disorders when drug therapy is ineffective [1]. To guide these interventional procedures, it is critical to localize the abnormalities accurately and rapidly by mapping the electrical activity. Conventional techniques are generally invasive and require a large number of electrodes to reconstruct the current field. Consequently, the procedure is time consuming and prone to artifacts [2-4]. To address these limitations, we have developed an alternative technique called ultrasound current source density imaging (UCSDI) [5-9], which potentially facilitates and enhances conventional electrical mapping. Potential advantages include 1) Fast, volume mapping of the current field using as few as one recording electrode and ground; 2) enhanced spatial resolution determined by the properties of the ultrasound beam; and 3) co-registration of UCSDI with anatomical ultrasound. Previous studies have demonstrated 4-D (volume + time) electric current mapping of a time-varying dipole in physiological saline [8]. Moreo-

ver, the technique is sensitive enough to detect and image current flow in the live rabbit heart with current densities on the order of 0.1 mA/cm^2 [9].

The principle of UCSDI is based on the AE effect, which is an interaction between the electric resistivity and acoustic pressure [10]. When an ultrasound beam intersects an electric current field, the ultrasound wave introduces a perturbation to the resistivity and hence generates an acoustoelectric (AE) voltage signal at the ultrasound frequencies [5-7]. The amplitude of the AE signal depends on the acoustic pressure, electric current density, and an interaction constant, which is an intrinsic parameter of the medium. For mapping the cardiac current density, the amplitude of the AE signal is on the order of 1 microvolt or less. Therefore, to optimize the signal-to-noise ratio (SNR), it is critical to consider the ultrasound parameters, such as frequency, pressure, focal zone size, and type of excitation. For the latter parameter, coded pulse waveforms, such as chirp pulses, have been implemented to improve SNR in ultrasonic and radar imaging systems for decades [14-15]. Waveforms that extend the time-bandwidth product of the ultrasound beam without sacrificing spatial resolution can improve the SNR [16-17]. In UCSDI, we have also demonstrated that chirp excitation can increase the SNR compared to wideband square pulse excitation by ~15dB [14] in phantoms. In this paper, we will test different coded excitation schemes to map the cardiac electric current distribution in live rabbit hearts. Moreover, we will implement the optimal scheme to map the cardiac activation wave using a clinical intracardiac catheter.

II. METHODS

Hearts were excised from white New Zealand rabbits and maintained alive for several hours using a standard Langendorff perfusion system (Radnoti LLC, Monrovia, Ca). A pair of bipolar simulating electrodes was in contact with the right atrium to pace the heart. The stimulation signal was a 1 msec square pulse produced by a function generator (Agilent, 33220A, Santa Clara, CA) at a repetition rate slightly higher than the natural beat rate of the heart. ECG and AE signals were recorded using either intramuscular or intracardiac electrodes. For intramuscular recording, AgCl/Ag wires were slightly poked into the left ventricle of

the heart (Fig. 1). For intracardial recording, a clinical catheter (CristaCath[TM] D-type, 36Y39R, Biosense Webster®) was inserted into the right ventricle. The ECG and AE signals were measured using the same electrodes and separated by different hardware filters. A spherically focused single element transducer (Panametrics V394, 1MHz, 38mm element diameter, 69mm focal length) was immersed in a water tank below the heart. The ultrasound beam was focused into the heart. The water was kept at a constant temperature of 37ºC. For wideband square pulse excitation, a pulse/receiver (5077PR, Panametrics) was used to drive the transducer and collect the pulse-echo (PE) signal. For frequency coded excitation, chirp signals with different pulse widths were produced by a function generator (Agilent, 33220A, Santa Clara, CA) and then amplified by a 300 W power amplifier (AG1021, T&C Power Conversion, Inc.). All PE, AE, and ECG signals were acquired by a National Instruments data acquisition system (NI-PXI 1042S). The timing between all instruments and the data acquisition system were well detailed in our previous work. [5].
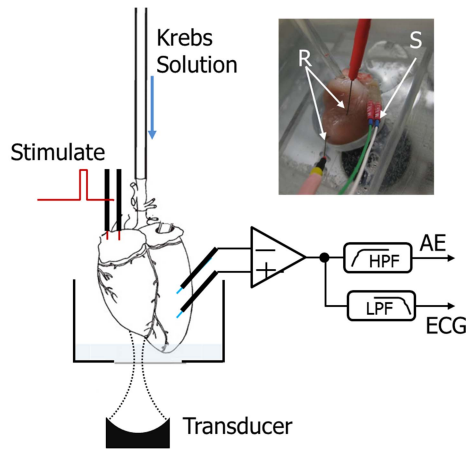

Fig. 1. Setup for applying UCSDI in the live rabbit heart prepared using a standard Langendorff procedure. Photo displays US transducer, tank, heart, recording (R) and stimulating (S) electrodes.

Pulse echo (PE) and AE signals were collected simultaneously every 400 µs during each cardiac cycle. All AE signals were converted into complex form and filtered using Hanning window in both slow physiologic and fast ultrasound time. The Hanning windows were matched to the frequency band of the ECG and frequency band of the ultrasound transducer.

The peak AE envelope was compared using different types of ultrasound excitation: short square pulse and chirps of different time duration T. A pulse compression algorithm was also employed to preserve the spatial resolution for chirp excitations. The details of the pulse compression algorithm for UCSDI were discussed in another study [18].

III. RESULTS

Fig. 2A depicts a typical ECG signal recorded from the epicardium of the isolated rabbit heart stimulated at the right atrium. The recording electrodes were placed in the wall of the left ventricle. Fig. 2B displays the filtered AE signals for square and chirp pulse excitation. The results indicate that with the same level of background noise, the AE signal produced using chirp excitation (T=20µs) is approximately twice as large as that of the square pulse excitation.
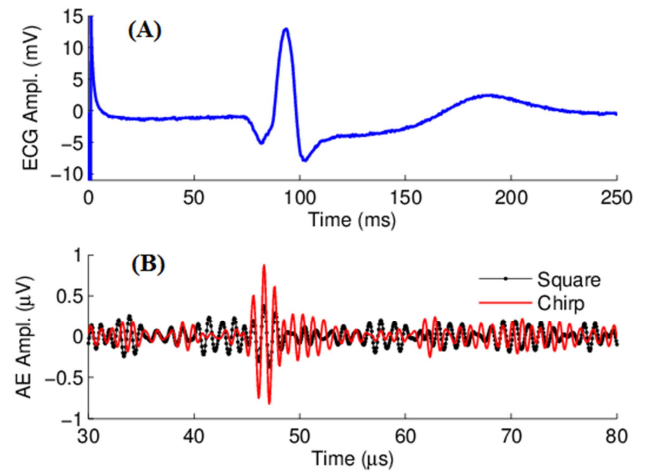

Fig. 2. (A) Typical ECG signal recorded using two needle electrodes in the left ventricle of a rabbit heart paced from the right atrium; (B) Typical filtered AE signals with 50 averages: the black dotted line represents the AE signal using square pulse excitation, whereas the red solid line denotes the AE signal using chirp pulse (T=20µs) excitation after pulse compression.

Fig. 3 presents M-mode UCSDI in the live rabbit heart acquired with different types of ultrasound excitation under the same conditions. The images confirm that chirp excitation yields higher contrast than short square pulse excitation. Also, the chirp pulse with the longer time duration T performs best.
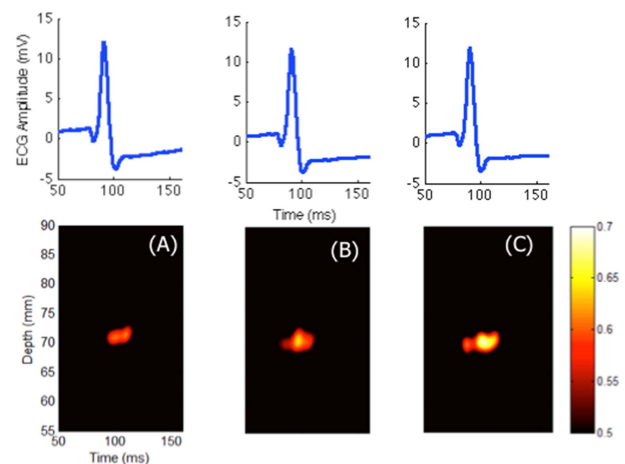

Fig. 3. Comparison of UCSDI M-mode images with different excitation schemes using the 1 MHz ultrasound transducer: Top row: ECG waveforms for each condition. (A) excited by a short square pulse matched to the center frequency of the transducer; (B) excited by a chirp pulse with T=10µs and (C) T=20µs. The images represent the envelope of the AE signals on linear scale; the units of the colorbar are in microvolts.

The SNRs of the three images in Fig. 3 were calculated using the peak and background values of each image. Based

on the results summarized in Fig. 4, the SNRs for frequency coded excitation were higher than for square pulse excitation, and the chirp pulse with the longer time duration (T=20µs) yielded the best SNR.
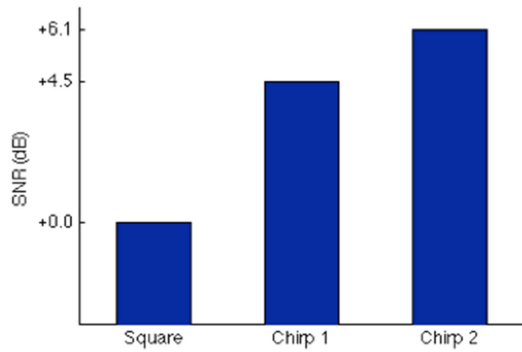

Fig. 4. SNR of the AE signal at the peak of the ECG using the three different US excitation schemes: 1) short square pulse, 2) chirp pulse 1 with $T = 10$µs and 3) chirp pulse 2 with $T = 20$µs.

The M-mode image acquired with the longer chirp pulse (T=20µs) is further demodulated to its baseband, which is displayed in Fig. 5A. The red or blue color of each pixel represents the polarity of the associated electric current at that position. An amplitude profile, drawn across the peak of the image (green dotted line in Fig. 5A), is displayed as a green dotted line in Fig. 5B. This AE amplitude profile at a particular depth roughly matches the recorded ECG signal (black solid curve in Fig. 5B) except for some high frequency noise.
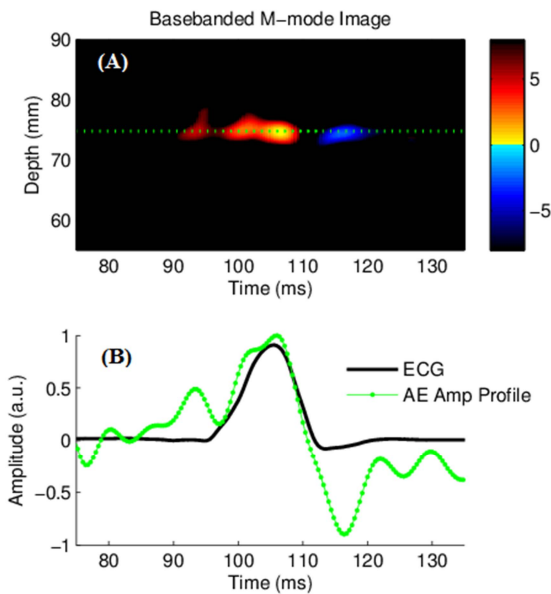

Fig. 5. (A) Basebanded (demodulated in fast time) M-Mode image recorded intramuscularly using two AgCl needle electrodes; the ultrasound transducer was excited by a chirp pulse with T = 20µs. (B) Recorded ECG signal (black solid curve) and an AE amplitude profile line across the peak of the M-mode image.

Next, the 7F clinical intracardiac catheter (Biosense Webster) was employed to mimic interventional conditions for electrical cardiac mapping. Instead of using the two needle recording electrodes as described previously, we recorded the AE signal on a pair of electrodes on the catheter. The optimal coded excitation (chirp $T = 20$µs), we conducted a B-scan along the short axis of the heart. The catheter was inserted into the right ventricle of the heart. To mitigate the heart movement during the scan, 2,3-butanedione monoxime (BDM) was added to the Krebs ringer solution to suppress the physical contractions of the heart. BDM decouples the mechanical and electrical cardiac events. At times immediately before and after the ECG, only background noise was observed. However, during the ECG waveform, regions of high current densities were observed in the heart near the catheter electrodes. A UCSDI B Mode image at the instant when the ECG reaches its peak is superimposed on the pulse echo image in Fig. 6. Strong AE signals appear in the heart wall at regions around the catheter. Because the catheter reflected ultrasound, no signal was observed on the far side of the catheter.
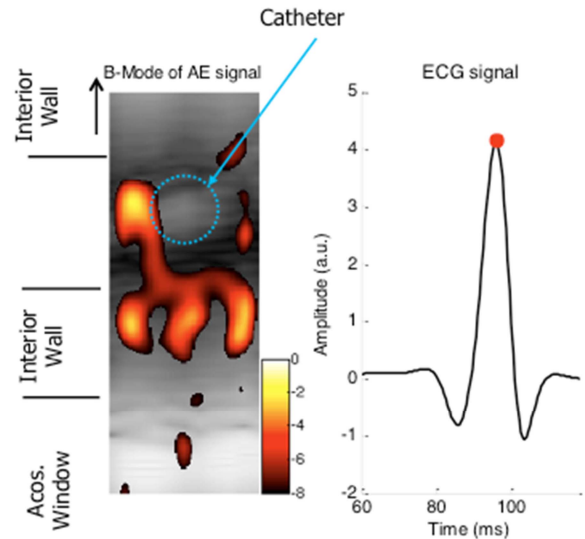

Fig. 6. (left) Superimposed pulse-echo (gray) and UCSDI (color) B-mode images (color) obtained in the live rabbit heart at the instant when the ECG signal (right) reached its peak (red dot).

IV. DISCUSSION AND CONCLUSION

In this paper, we studied UCSDI in live rabbit hearts using frequency coded ultrasound excitation. We found that chirp pulses of $T = 10$ μs and $T = 20$ μs yielded better SNR than the square pulse by 4.5 dB and 6.1 dB, respectively. Using the chirp pulse of $T = 20$μs, we were able to image cardiac current in the rabbit heart using both intramuscular (AgCl needle electrodes) and intracardiac (clinical catheter) recording. From UCSDI M-mode images at a single ultrasound location, we demonstrated that local current density near the ultrasound focus followed the timing of the ECG signal. Moreover, from the UCSDI B-mode image obtained using a clinical intracardiac catheter, we demonstrated that time-varying current densities could be mapped at different spatial locations by simply scanning the ultrasound beam.

Further optimization of the ultrasound and electrode parameters, along with other noise reduction techniques, will facilitate translation of UCSDI to the clinic for the diagnosis and treatment of arrhythmia and epilepsy.

REFERENCE

[1] W.M. Jackman, X.Z. Wang, K.J. Friday, C.A. Roman, K.P. Moulton, K.J. Beckman, et al, "Catheter Ablation of Accessory Atrioventricular Pathways (Wolff-Parkinson-White Syndrome) by Radiofrequency Current," *New England Journal of Medicine*, 324(23): pp. 1605-1611, 1991.

[2] H.U. Klemm, D. Steven, C. Johansen, R. Ventura, T. Rostock, B. Lutomsky, et al, "Catheter motion during atrial ablation due to the beating heart and respiration: Impact on accuracy and spatial referencing in three-dimensional mapping," *Heart Rhythm*, vol. 4, pp. 587–582, 2007.

[3] J. J. Goldberger, "Atrial fibrillation ablation: Location, location, location," *J. Cardiovasc. Electrophysiol*., vol. 17, pp. 1271–1273, 2006.

[4] R. Malkin, N. Kramer, B. Schnitz, M. Gopalakrishnana, and A. Curry,"Advances in electrical andmechanical cardiac mapping," *Physiol. Meas*., vol. 26, pp. R1–R14, 2005.

[5] R. Olafsson, R. S. Witte, C. Jia, S.-W. Huang, and M. O'Donnell, "Detection of Electrical Current in a Live Rabbit Heart using Ultrasound," in 2007 *IEEE Ultrasonics Symposium*, New York, NY, pp. 989-992, 2007.

[6] R. S. Witte, R. Olafsson, S. W. Huang, and M. O'Donnell, "Imaging current flow in lobster nerve cord using the acoustoelectric effect," *Appl. Phys. Lett*., vol. 90, pp. 163902, 2007.

[7] R. Olafsson, R. S. Witte, S.-W. Huang, and M. O'Donnell, "Ultrasound Current Source Density Imaging," *IEEE Trans. on Biomedical Engineering*, vol. 55, pp. 1840-1848, 2008.

[8] Z.H. Wang, R. Olafsson, P. Ingram1, Q. Li, Y. Qin, and R.S. Witte, "Four-dimensional ultrasound current source density imaging of a dipole field," *Appl. Phys. Lett*. 99, 113701 2011.

[9] R. Olafsson, R.S. Witte, C.X. Jia, S.W. Huang, K. Kim, and M. O'Donnell, "Cardiac Activation Mapping Using Ultrasound Current Source Density Imaging (UCSDI)," *IEEE Transactions on Ultrasonics Ferroelectrics and Frequency Control*, vol. 56, pp. 565-574, 2009.

[10] R. H. Parmenter, "The Acousto-Electric Effect," *Phys. Rev*. 89, pp. 990–998, 1953.

[11] J. Jossinet, B. Lavandier, and D. Cathignol, "The phenomenology of acousto-electric interaction signals in aqueous solutions of electrolytes," *Ultrasonics*, vol. 36, pp. 607-613, 1998.

[12] F.S. Foster and J.W. Hunt, "The design and characterization of short pulse ultrasound transducers," *Ultrasonics*, pp. 116, 1978.

[13] R. Yang, X. Li, J. Liu and B. He, "3D current source density imaging based on the acoustoelectric effect: a simulation study using unipolar pulses," *Phys. Med. Biol*. Vol. 56, pp. 3825–3842, 2011.

[14] O'Donnell, M., "Coded Excitation System for Improving the Penetration of Real-Time Phased-Array Imaging-Systems," *IEEE Transactions on Ultrasonics Ferroelectrics and Frequency Control*, 39(3), pp. 341-351, 1992.

[15] E. Brookner, "Phased-Array Radars," *Scientific American*, 252(2), pp. 94-102, 1985.

[16] N. A. H. K. Rao, "Investigation of a pulse compression technique for medical ultrasound: A simulation study," *Med. Biol. Eng. Comp*., 32(2), pp. 181–188, 1994.

[17] T. Misaridis and J. A. Jensen, "Use of Modulated Excitation Signals in Medical Ultrasound," *IEEE Transactions on Ultrasonics, Ferroelectrics, and Frequency Control*, 52(2), pp. 177, 2005.

[18] Y. Qin, Z. Wang, P. Ingram, Q. Li, and R. Witte, "Optimizing Frequency and Pulse Shape for Ultrasound Current Source Density Imaging," *IEEE Transactions on Ultrasonics Ferroelectrics and Frequency Control*, [In press].